ELSEVIER

Synthesis and gas chromatographic evaluation of a high-temperature hydrogen-bond acid stationary phase

Sophie D. Martin[a], Colin F. Poole[a],*, Michael H. Abraham[b]

[a]*Department of Chemistry, Rm. 171, Wayne State University, Detroit, MI 48202, USA*
[b]*Department of Chemistry, University College London, 20 Gordon Street, London, WC1H OAJ, UK*

Abstract

A new high-temperature hydrogen-bond acid stationary phase, PSF6, consisting of a poly(methylsiloxane) backbone with 2-(4-butanephenyl)-1,1,1,3,3,3-hexafluoropropan-2-ol substituent groups is described for gas–liquid chromatography. PSF6 has a low cohesive energy [similar to poly(methylphenylsiloxane)s], is moderately dipolar, has no hydrogen-bond basicity, and is a strong hydrogen-bond acid. The hydrogen-bond acidity of the stationary phase is shown to be strongly temperature dependent but remains significant up to temperatures of about 200°C. A comparison of the solvent properties of PSF6 with 12 common poly(siloxane) stationary phases indicates its singularity and usefulness for selectivity optimization in method development. © 1998 Elsevier Science B.V.

Keywords: Stationary phases, GC; Poly(methylsiloxane); Hydrogen-bond acids

1. Introduction

A very large number of stationary phases have been employed in gas–liquid chromatography, and with the few exceptions noted below, none are significant high-temperature hydrogen-bond acids [1–4]. The general reason for this is that most common hydrogen-bond acid solvents, such as alcohols and phenols, are simultaneously strong hydrogen-bond bases, and prefer to form self-association hydrogen-bond complexes rather than to interact with solute molecules.

To understand the context of this paper it is important to appreciate the difference between hydrogen-bond acidity and proton-transfer acidity. The two are separate concepts. The proton-transfer acidi-

ty is indicated by the hydrogen ion concentration (activity) resulting from bond breaking and is largely determined by the stability of the conjugate base. The hydrogen-bond acidity does not involve ion formation; it is an intermolecular interaction in which a bond-restrained hydrogen atom is shared with an electronegative atom from another solute or solvent molecule forming a reversible chemical bond [5,6]. The positively charged hydrogen atom is said to come from the molecule that is a hydrogen-bond donor (or acid) but remains covalently bonded to the rest of the molecule and is shared with a second molecule referred to as a hydrogen-bond acceptor (or base). Hydrogen bonds are rapidly made and broken and are important contributors to selective solute–solvent interactions belaying our interest in their exploitation for methods development in gas–liquid chromatography. This desire is only mitigated by the

*Corresponding author

lack of suitable solvents for use at temperatures of interest for gas chromatographic separations.

The identification of stationary phases with significant hydrogen-bond acidity requires a model capable of separating this interaction from all other concurrent intermolecular interactions. The solvation parameter model serves this purpose in chromatography and other equilibrium processes characterized by a free energy [5,7–10]. The model is set out below in a form suitable for gas–liquid chromatography:

$$\log K_{L} = c + l \log L^{16} + rR_2 + s\pi_2^{H} + a\sum \alpha_2^{H}$$
$$+ b\sum \beta_2^{H} \qquad (1)$$

where $\log K_{L}$ is the gas–liquid distribution constant and the solute descriptors are $\log L^{16}$ the distribution constant for the solute between a gas and n-hexadecane at 298 K, R_2 excess molar refraction (in cm^3/10), π_2^{H} the ability of the solute to stabilize a neighboring dipole by virtue of its capacity for orientation and induction interactions, $\Sigma \alpha_2^{H}$ and $\Sigma \beta_2^{H}$ the solute's effective hydrogen-bond acidity and effective hydrogen-bond basicity, respectively. The solute's excess molar refraction is usually available by simple arithmetic calculation; the other solute descriptors are derived from equilibrium measurements for complexation and partition processes with values available for over 2000 compounds. The system constants in Eq. (1) are defined by their complementary interactions to the solute descriptors: the r constant refers to the capacity of the solvent for interaction with solute n- or π-electrons; the s constant to the solvent's capacity for dipole–dipole and dipole-induced dipole interactions; the a constant characterizes the solvent's hydrogen-bond basicity (because a basic solvent will interact with an acidic solute); the b constant the solvent's hydrogen-bond acidity; and the l constant incorporates contributions from solvent cavity formation and dispersion interactions. The system constants are determined by multiple linear regression analysis of experimental $\log K_{L}$ values for a group of solutes of sufficient number and variety to establish the statistical and chemical validity of the model, without cross-correlation between the chosen descriptors, and with an absence of clustering for individual descriptors.

The hydrogen-bond acidity of a stationary phase is indicated by the magnitude of the b system constant in Eq. (1). To maximize selectivity stationary phases with a large b system constant and minimal capacity for other polar interactions, corresponding to small a, r and s system constants, are preferred. In particular the ratio of the b/a system constants should be as large as possible to minimize the tendency for self-association. Based on the collection of retention data by McReynolds for 77 stationary phases at 120°C [11], of Laffort et al. for five stationary phases at 60°C [12], of Poole et al. for 24 stationary phases at 121°C [13], of Abraham et al. for four substituted amides at between 25 and 100°C [14], and of Berthold et al. for 19 chiral stationary phases (17 of which are cyclodextrins) at 100°C [15], Abraham could identify only five solvents (docosanol, diglycerol, sorbitol, and two cyclodextrins) with weak hydrogen-bond acid properties (Table 1). These five alcohol-containing solvents are, in fact, stronger hydrogen-bond bases than they are acids and, in addition, are appreciably dipolar. None of these solvents would qualify as selective hydrogen-bond acid stationary phases as well as possessing a limited temperature operating range. Poole and co-workers [16–19] have evaluated a large number of stationary phases with functional groups anticipated to function as hydrogen-bond acid solvents, including N,N,N',N'-tetrakis (2-hydroxypropyl)ethylenediamine, poly(ethylene glycols), tetra-n-butylammoniumN,N-(bis-2-hydroxyethyl)-2-aminoethanesulfonate, di(2-ethylhexyl)phosphoric acid and various liquid organic salts containing alcohol, amine, amide and phenol groups. These stationary phases did not act as hydrogen-bond acids at 121°C, except for two liquid organic salts (out of 50) containing a hydroxypyridinium cation, which were weak hydrogen-bond acids (Table 1). Occasionally, weak hydrogen-bond acid properties have been indicated for poly(siloxane) and poly(ester) stationary phases, but this has always been traced to hydrolysis or oxidation impurities in the polymers [19,20].

Using a model similar to the solvation parameter model but employing a different set of solute descriptors, Carr and co-workers [21–23] studied 21 representative stationary phases from McReynolds' 77-phase set, Poole's 24-phase set, and eight common stationary phases available for open tubular columns, reaching the same conclusion as discussed

Table 1
System constants for hydrogen-bond acid stationary phases used in gas–liquid chromatography

Solvent	Temperature (°C)	System constants				
		r	s	a	b	l
Docosanol	80	0.16	0.31	1.56	0.45	0.72
	100	0.15	0.30	1.13	0.39	0.66
Diglycerol	120	0.55	1.63	2.77	0.52	0.23
Sorbitol	120	0.35	0.81	1.77	0.34	0.36
Permethylated S-hydroxypropyl-α-cyclodextrin	100	0.25	0.67	1.41	0.29	0.57
Permethylated S-hydroxypropyl-γ-cyclodextrin	100	0.25	0.67	1.31	0.48	0.49
1-Ethyl-3-hydroxypyridinium 4-toluenesulfonate	120	0.45	1.96	2.89	0.37	0.31
1-Ethyl-3-hydroxypyridinium bromide	120	0.50	2.11	3.21	0.32	0.24
4-Dodecyl-α,α-bis(trifluoromethyl)-benzyl alcohol	80	-0.22	0.48	0	2.69	0.68
3-Pentadecylphenol[a]	110		0.66	0.29	1.46	0.60
1,1,1-Trifluoro-2-eicosanol*	70		0.56	0.48	1.58	0.74
N-Tetradecyl-1,1,1-trifluoroacetamide[a]	80		0.90	0.78	0.66	0.67
Bis(3-allyl-4-hydroxyphenyl)sulfone	120[b]	-0.05	1.32	1.27	1.46	0.42
	176	0.17	1.16	0.81	1.29	0.33

[a]Results using the solvation parameters proposed by Li et al. [25].
[b]Supercooled liquid state.

above, that there are no useful high-temperature hydrogen-bond acid stationary phases commonly employed in gas–liquid chromatography. The model they used is given below:

$$\log K_{L} = c + l \log L^{16c} + d\delta_2 + s\pi_2^c + a\alpha_2^c + b\beta_2^c \tag{2}$$

where the system constants and solute descriptors have their usual meaning except for δ_2 which is an empirical polarizability correction factor (used in place of R_2). The superscript c is used to indicate that the solute descriptors are derived from chromatographic data and generally have different numerical values to the solute descriptors used in Eq. (1). Carr and co-workers [24,25] evaluated five low-molecular-weight carboxylic acid and fluorine-containing alcohols in their search for a strong hydrogen-bond acid stationary phase to define a scale of solute hydrogen-bond basicity (β_2^c). Stearic acid and N-tetradecyl-1,1,1-trifluoroacetamide were only weak hydrogen-bond acids, but the two fluorine-containing alcohols, 4-dodecyl-α,α-bis(trifluoromethyl)benzyl alcohol and 1,1,1-trifluoro-2-eicosanol, and the phenol 3-pentadecylphenol had favorable properties (Table 1). 4-Dodecyl-α,α-bis-(trifluoromethyl)benzyl alcohol is one of the strongest hydrogen-bond acid solvents shown in

Table 1 and, most importantly in terms of selectivity, has no hydrogen-bond basicity. Unfortunately, this solvent is quite volatile, and required presaturation of the carrier gas with stationary phase for use at temperatures as low as 80°C. From previous studies of sensor coatings, Abraham et al. [26] suggested bis(3-allyl-4-hydroxyphenyl)sulfone as a high-temperature hydrogen-bond acid stationary phase. Again this stationary phase had favorable hydrogen-bond acidity (Table 1), but was restricted in use to the temperature range 150–220°C by its melting point (lower temperature) and volatility (upper temperature) [27].

A number of nerve gases and toxic chemicals are strong hydrogen-bond bases, and hydrogen-bond acid sensor coatings have been sought for their selective detection. Abraham and co-workers characterized 13 liquids containing the 4,4′-isopropylidenediphenol group for use as sensor coatings, of which seven were prepared in anticipation of possessing significant hydrogen-bond acid properties [26]. In each case the hydrogen-bond acid site was the phenol group with the strongest hydrogen-bond acid solvents identified as 2,2-bis(3-allyl-4-hydroxyphenyl)hexafluoropropane (I), 2,2-bis(4-hydroxy-3-propylphenyl)hexafluoropropane (II), 2,2′-diallyl-4,4′-isopropylidenediphenol (III), and 2,2′-dipropyl-4,4′-isopropylidenediphenol (IV) (Table 2, Fig. 1).

Table 2
System constants for hydrogen-bond acid solvents used as sensor coatings

Solvent[a]	Temperature (°C)	System constants				
		r	s	a	b	l
I	25	−0.48	1.04	0.89	4.56	0.86
II	25	−0.38	1.38	0.71	5.31	0.98
III	25	−0.92	2.24	2.79	2.41	0.98
IV	25	−1.20	1.88	2.84	2.86	1.19
V	25	−0.47	0.60	0.70	4.25	0.72
VI	25	−0.89	1.70	1.16	4.32	0.68
VII	25	−0.74	0.61	1.44	3.67	0.71
	60	−0.73	0.81	0.76	2.72	0.56
VIII	25	−0.67	1.45	1.49	4.09	0.81
	60	−0.46	1.15	0.91	2.65	0.61
	90	−0.63	1.37	0.61	0.88	0.39

[a] See Fig. 1 for identification and structures.

For structurally related coatings replacing a methyl group by the trifluoromethyl group resulted in an increase in the hydrogen-bond acidity of the coating, and a decrease in its hydrogen-bond basicity and
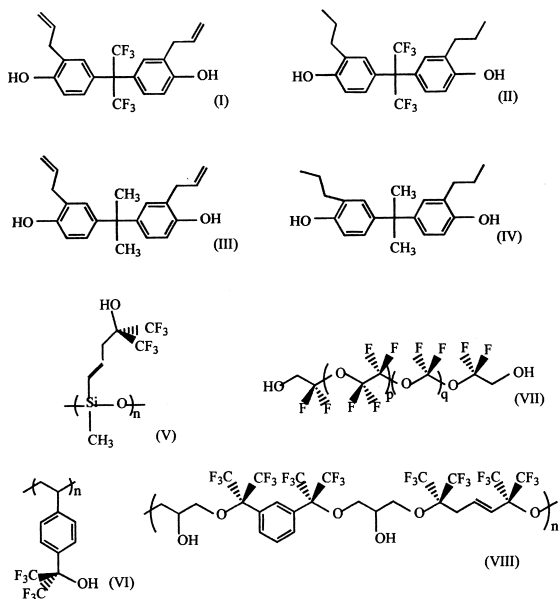

Fig. 1. Structures of solvents used as hydrogen-bond acid sensor coatings. 2,2-Bis(3-allyl-4-hydroxyphenol)hexafluoropropane (I), 2,2-bis(4-hydroxy-3-propylphenyl)hexafluoropropane (II), 2,2′-diallyl-4,4′-isopropylidenediphenol (III), 2,2′-dipropyl-4,4′-isopropylidenediphenol (IV), poly(oxy{methyl[4-hydroxy-4,4-bis-(trifluoromethyl)but-1-en-1-yl]silylene}) (V), poly{1-[4-(2-hydroxy-1,1,1,3,3,3-hexafluoroprop-2-yl)phenyl]ethylene} (VI), Fomblin Z-DOL (VII), and Fluoropolyol (VIII).

capacity for dipole-type interactions, thus increasing its selectivity as a hydrogen-bond acid solvent. Abraham and co-workers [28,29] also characterized the sorption properties of the four fluorine-containing polymers poly(oxy{methyl[4-hydroxy-4,4-bis(trifluoromethyl)but-1-en-1-yl]silylene}) (V), poly{1-[4-(2-hydroxy-1,1,1,3,3,3-hexafluoroprop-2-yl)phenyl]-ethylene} (VI), Fomblin Z-DOL (VII), and Fluoropolyol (VIII), again with a view to their use as chemically selective hydrogen-bond acid sensor coatings (Table 2, Fig. 1). All four polymers contain fluorine-activated alcohol groups as the hydrogen-bond acid center; all four are strong hydrogen-bond acids; (V) is a comparatively weak hydrogen-bond base compared to the other polymers (which are moderate hydrogen-bond bases); (V) and (VII) have low dipolarity, while the other polymers are moderately dipolar. Polymers (VI) [30], (VII) [31], and (VIII) [32] have been used to fabricate sensors, while (V) shows desirable properties for such applications. Coatings for chemical sensors are generally optimized for use at temperatures close to room temperature, so the properties of these materials at higher temperatures are generally unknown. In the case of (VII) and (VIII) some limited temperature data are available (Table 2), and demonstrate a significant decline in hydrogen-bond acidity at higher temperatures. The glass transition temperature or melting point, viscosity, and chemical stability of these polymers casts doubt on whether they would be useful as high-temperature hydrogen-bond acid stationary phases for gas–liquid chromatography.

Poly(siloxane)s are the most popular stationary phases for gas–liquid chromatography on account of their wide operating temperature range (low temperature glass transition point, low vapor pressure, and high thermal stability), favorable diffusion and solubility of many solute types, chemical inertness, favorable wetting characteristics (important in coating low energy surfaces), wide range of chromatographic selectivity (achieved through substitution of different functional groups onto the siloxane backbone), and ease of immobilization for applications employing open tubular columns [1,33]. As a generic strategy for the synthesis of high-temperature hydrogen-bond acid stationary phases we propose to employ poly(siloxane)s as the solvent backbone and tether selected fluorine-containing alcohol or phenol substituents to it in order to obtain the desired hydrogen-bond acid properties. Initial studies have been performed with a 4-(2-hydroxy-1,1,1,3,3,3-hexafluoroprop-2-yl)phenyl hydrogen-bond acid center attached to a poly(methylsiloxane) backbone by a butane spacer arm. The polymer synthesized is shown in Fig. 2, and will be referred to as PSF6 in the text, as well as a non-fluorine containing analog, PSH, prepared to evaluate the contribution of the electron-withdrawing fluorine groups to the polarity (capacity for hydrogen-bond acid, hydrogen-bond base and dipole-type interactions) of the stationary phase. An important precept of this work is that incorporation of fluorine into the alcohol group will increase the hydrogen-bond acidity of the alcohol
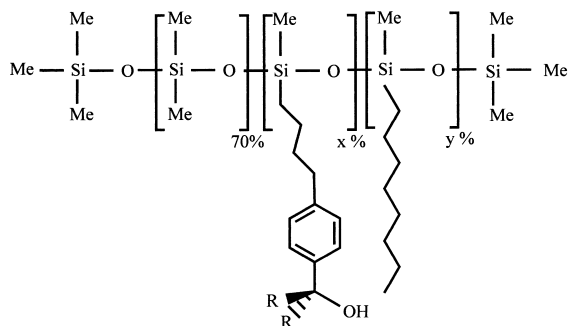
group and simultaneously reduce its hydrogen-bond basicity so that the poly(siloxane) stationary phase will exhibit a favorable selectivity for hydrogen-bond acid interactions with a minimum tendency to self-associate. The non-fluorine-containing analog by contrast is expected to be less useful as a hydrogen-bond acid stationary phase and exhibit significant self-association complexation because of its higher hydrogen-bond basicity. Thus, it provides a test of the validity of the general case for the development of high-temperature hydrogen-bond acid stationary phases based on the incorporation of fluorine-containing alcohol and phenol groups into a poly(siloxane) backbone.

2. Experimental

All solvents were OmniSolv grade from EM Science (Gibbstown, NJ, USA). 4-Bromobenzyl bromide, magnesium turnings, 1.7 *M* tert.-butyllithium in hexane, 1,1,1,3,3,3-hexafluoro-acetone, 1,1,1,3,3,3-hexamethyldisilazane, trimethyl-chlorosilane, imidazole, hydrogen hexachloroplatinate (IV) hydrate, 1-octene, tetrabutylammonium fluoride (1.0 *M* solution in tetrahydrofuran) were obtained from Aldrich Chemical Co. (Milwaukee, WI, USA). Allyl bromide was obtained from Across Organics (Pittsburgh, PA, USA) and methylhydrosiloxanedimethylsiloxane copolymer containing 25–30% silane from Gelest, Inc. (Tullytown, PA, USA). Silica gel (74–177 μm) for column chromatography and silica gel 60 F$_{254}$ precoated thin-layer chromatography plates were obtained from J.T. Baker (Danvers, MA, USA). Chromosorb W-AW (177–250 μm) and silanized glass wool was obtained from Anspec (Ann Arbor, MI, USA). Other solutes used for solvent characterization by gas chromatography were obtained from several sources and were of the highest purity generally available.

2.1. Synthesis of poly(oxy{methyl[4-(2-hydroxy-1,1,1,3,3,3-hexafluoroprop-2-yl)phenyl]butyl}-silylene)-co-oxy(dimethylsilylene)

Reaction flasks and associated equipment were dried at 120°C for several hours (or overnight) and

Fig. 2. Structures of poly(oxy{methyl[4-(2-hydroxy-1,1,1,3,3,3-hexafluoroprop - 2 - yl)phenyl]butyl}silylene)-*co*-oxy(dimethylsilylene) with R = CF$_3$ and Me = CH$_3$, PSF6, and poly(oxy{methyl-[4 - (2-hydroxyprop-2-yl)phenyl]butyl}silylene) - *co* - oxy(dimethylsilylene) with R = Me = CH$_3$, PSH.

assembled as indicated under dry nitrogen. 4-Bromo-benzyl bromide was recrystallized from methanol prior to use. Tetrahydrofuran was freshly distilled from sodium metal prior to use. Diethyl ether was dried over anhydrous sodium sulfate. A general outline of the synthetic route for the preparation of PSF6 and PSH is given in Fig. 3.

2.1.1. 4-(4-Bromophenyl)-1-butene

To a 100-ml three-necked flask containing a magnetic stirring bar with dropping funnel and reflux condenser was added 0.721 g (29.7 mmol) of magnesium turnings, 2 ml of diethyl ether and a crystal of iodine. The mixture was gently warmed under nitrogen and 7.50 g (30 mmol) of 4-bromo-benzyl bromide in 10 ml of diethyl ether added dropwise to maintain a gentle reflux. After all of the 4-bromobenzyl bromide had been added, the mixture was cooled to −15°C (ice–methanol slush bath), and 3.63 g (30 mmol) of allyl bromide in 10 ml of diethyl ether was added dropwise over 20 min. After 1 h, the diethyl ether was removed by evaporation, 30 ml of benzene added, the mixture heated to reflux for 1 h, cooled, and then poured into 50 ml of 4 M

hydrochloric acid. The aqueous phase was neutralized with a saturated solution of sodium bicarbonate and the organic phase removed in a separating funnel. The aqueous layer was extracted twice with ethyl acetate. the organic phases combined, dried over anhydrous sodium sulfate, filtered through a sintered glass funnel, and then concentrated under reduced pressure to yield a pale yellow oil. The oil was distilled at 52–54°C and 0.2 mmHg to yield 2.31 g (43%) of 4-(4-bromophenyl)-1-butene as a colorless oil (lit. 65–67°C at 0.6 mmHg [34]). ^{1}H NMR (ppm): 2.3 (quartet, 2H); 2.6 (triplet, 2H); 4.9 (multiplet, 2H); 5.8 (multiplet, 1H); 7.0 (doublet, 2H); and 7.4 (doublet, 2H). ^{13}C NMR (ppm): 34.8; 35.3; 115.3; 119.6; 130.2; 131.3; 137.6; and 140.8. FTIR (cm^{-1}): 3078; 2978; 2929; 2856; 1640; 1488; 1452; 1440; 1403; 1111; 1072; 1011; 995; 913; 840; 803; 771; and 644.

2.1.2. 2-(4-But-3-enyl-phenyl)-1,1,1,3,3,3-hexa-fluoropropan-2-ol

To a 100-ml three-necked round bottom flask with magnetic stirring bar fitted with a septum seal and a gas inlet tube was added a dry ice condenser (center
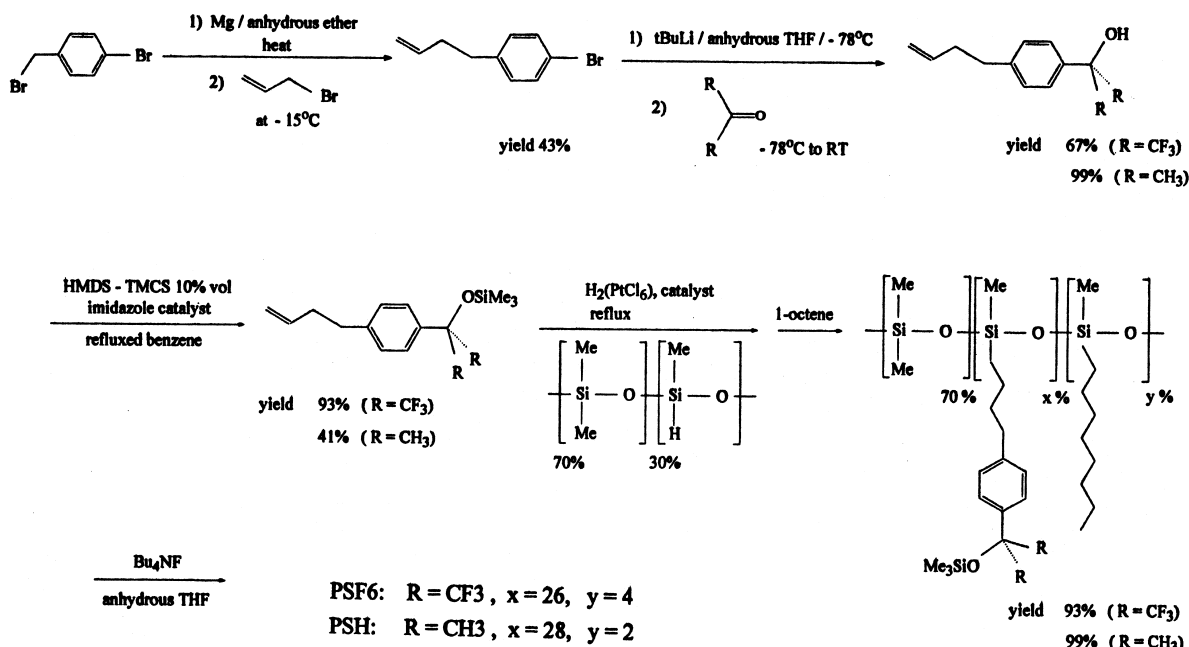

Fig. 3. Schematic diagram of the reaction steps for the synthesis of PSF6 and PSH.

neck) connected to a hexylamine trap and nitrogen bubbler in series. The flask was charged with 2.20 g (10.4 mmol) of 4-(4-bromophenyl)-1-butene in 50 ml of tetrahydrofuran, cooled to $-78°C$ (dry ice–acetone bath), and 12.5 ml of 1.7 *M tert*-butyllithium (21.3 mmol) in hexane was added by syringe. The reaction mixture was stirred at $-78°C$ for 30 min, at which point the mixture had turned dark orange–red. Hexafluoroacetone was slowly bubbled into the mixture until the solution became pale yellow, the dry ice–acetone bath was then removed, and the solution allowed to warm up to room temperature over about 2 h. The solvent was removed under reduced pressure and the reaction residue washed with a saturated solution of ammonium chloride, the organic layer collected, and the aqueous phase extracted with ethyl acetate. The organic phases were combined, dried over anhydrous sodium sulfate, the solvent removed under reduced pressure, and the yellow oil purified by flash chromatography over silica gel with hexane–ethyl acetate (20:1, v/v) as mobile phase to give 2.07 g (67%) of 2-(4-but-3-enyl-phenyl)-1,1,1,3,3,3-hexafluoropropan-2-ol [30]. ^{1}H NMR (ppm): 2.4 (quartet, 2H); 2.7 (triplet, 2H); 3.4 (singlet, 1 OH); 5.0 (multiplet, 2H); 5.88 (multiplet, 1H); 7.3 (doublet, 2H); and 7.6 (doublet, 2H). ^{13}C NMR (ppm): 34.9; 35.0; 115.2; 120.7; 124.6; 126.4; 127.3; 128.6; 137.6; and 144.2. ^{19}F NMR (ppm): -75.47 (singlet). FTIR (cm^{-1}): 3500 (broad); 3046; 3003; 2982; 2932; 2861; 1641; 1616; 1517; 1442; 1421; 1365; 1328; 1269; 1214; 1166; 1105; 1023; 995; 949; 923; 817; 751; 708; and 644.

2.1.3. 2-(4-But-3-enyl-phenyl)-1,1,1,3,3,3-hexafluoro-2-trimethylsiloxypropane

To a 250-ml three-necked round-bottomed flask with magnetic stirring bar, two septum seals and a reflux condenser on the center neck connected to a nitrogen bubbler, was added 4.76 g (16.0 mmol) of 2-(4-but-3-enyl-phenyl)1,1,1,3,3,3-hexafluoropropan-2-ol in 10 ml of benzene, 3.4 ml (16.1 mmol) of 1,1,1,3,3,3-hexamethyldisilazane (HMDS), 340 μl (10% of HMDS by volume) trimethylchlorosilane, and 1.05 g (15.4 mmol) of imidazole in 2 ml of benzene. The mixture was refluxed for 1 h, cooled, and extracted with water at pH 6. The aqueous phase was extracted with ethyl acetate, the organic phases combined, dried over sodium sulfate, and the solvent

removed under reduced pressure to give 5.49 g (93%) of the trimethylsilyl ether.

2.1.4. Poly(oxy{methyl[4-(2-hydroxy-1,1,1,3,3,3-hexafluoroprop-2-yl)phenyl]butyl}silylene)co-oxy(dimethylsilylene)

In a 100-ml three-necked round-bottomed flask with magnetic stirring bar, two septum seals and a reflux condenser on the center neck connected to a nitrogen bubbler was added 3.47 g (9.38 mmol) of monomer and 2.08 g of poly(dimethylmethyl-hydrosiloxane) in 6 ml of benzene. The solution was heated to reflux and 100 μl of a fresh solution of (7.4 mmol) hydrogen hexachloroplatinate (IV) hydrate in 2-propanol was added. A further 100 μl of the same solution was added in increments over 5 h. The solution turned black. The disappearance of the Si–H bond was followed by NMR. Once the Si–H bond had disappeared, 80 μl (0.051 mmol) of 1-octene was added to quench the reaction and the solution refluxed for a further 6 h. The mixture was cooled and 10 g of ammonium chloride and 1 ml of 37% HCl in 10 ml of water added, the mixture stirred for 2 h, the organic phase separated, and the aqueous phase filtered through a sintered glass funnel and extracted with ethyl acetate. The organic phases were combined, dried over sodium sulfate and the solvent removed under vacuum to give 5.17 g (93%) of the trimethylsilyl-protected polymer.

To the trimethylsilyl-protected polymer in 6 ml of tetrahydrofuran was added 8.9 ml of 1.0 *M* tetrabutylammonium fluoride solution in tetrahydrofuran, and the mixture stirred for 0.5 h at room temperature. The solvent was removed under vacuum, and the residue extracted with ethyl acetate. The organic phase was washed six times with 100 ml of distilled water, dried over anhydrous sodium sulfate, and the solvent evaporated under vacuum to give 4.64 g of PSF6. ^{1}H NMR (ppm): 0.05 (singlet, 9H); 0.5 (multiplet, 2H); 1.3 (multiplet, 2H); 1.6 (multiplet, 2H); 2.6 (multiplet, 2H); 3.0 (broad, 1 OH); 7.2 (doublet, 2H); and 7.6 (doublet, 2H). ^{13}C NMR (ppm): -0.7; 0.7; 1.0; 1.7; 16.88; 22.6; 34.4; 35.2; 120.7; 124.6; 126.4; and 128.6. ^{19}F NMR (ppm): -75.77 (singlet). FTIR (cm^{-1}): 3600; 3500 (broad); 2961; 2932; 2860; 1616; 1517; 1412; 1261; 1076; 973; 924; 842; 805; and 708.

2.2. Synthesis of poly(oxy{methyl[4-(2-hydroxyprop-2-yl)phenyl]butyl}silylene)-co-oxy(dimethylsilylene)

2.2.1. 2-(4-But-3-enyl-phenyl)propan-2-ol

To a 100-ml three-necked round-bottomed flask with magnetic stirring bar fitted with a septum seal and a gas inlet tube was added a water-circulating condenser (center neck) connected to a nitrogen bubbler. The flask was charged with 6.59 g (31.2 mmol) of 4-(4-bromophenyl)-1-butene in 30 ml of tetrahydrofuran, cooled to −78°C (dry ice–acetone bath), and 42 ml of 1.5 M tert-butyllithium (63 mmol) in hexane was added by syringe. The reaction mixture was stirred at −78°C for 30 min, at which point the mixture had turned dark orange–red. Acetone (20 ml, 438 mmol) was slowly added by syringe, the dry ice–acetone bath was then removed, and the solution allowed to warm up to room temperature over about 2 h. The solvent was removed under reduced pressure and the reaction residue poured into 100 ml of 2 M HCl, the organic layer separated, the aqueous solution extracted with ethyl acetate, and the combined organic phases washed with a saturated solution of sodium bicarbonate. The organic phase was dried over anhydrous sodium sulfate, the solvent removed under reduced pressure, and the yellow oil purified by flash chromatography over silica gel with hexane–ethyl acetate (20:1, v/v) as mobile phase to give 5.88 g (99%) of 2-(4-but-3-enyl-phenyl)propan-2-ol [30]. ^{1}H NMR (ppm): 1.59 (singlet, 6H); 2.1 (singlet, 1 OH); 2.4 (quartet, 2H); 2.7 (triplet, 2H); 5.0 (multiplet, 2H); 5.88 (multiplet, 1H); 7.18 (doublet, 2H); and 7.42 (doublet, 2H). ^{13}C NMR (ppm): 31.7; 34.9; 35.5; 72.4; 114.9; 124.4; 126.4; 128.2; 128.6; 138.1; 140.2; and 146.7. FTIR (cm^{−1}): 3394 (broad); 3077; 3024; 2976; 2928; 2857; 1640; 1511; 1446; 1410; 1364; 1259; 1169; 1097; 996; 954; 910; 863; and 734.

2.2.2. 2-(4-But-3-enyl-phenyl)-2-trimethyl-siloxypropane

To a 250-ml three-necked round-bottomed flask with magnetic stirring bar, two septum seals and a reflux condenser on the center neck connected to a nitrogen bubbler, was added 5.88 g (30.9 mmol) of 2-(4-but-3-enyl-phenyl)propan-2-ol in 10 ml of N,N-dimethylformamide, 4 ml (18.9 mmol) of 1,1,1,3,3,3-hexamethyldisilazane (HMDS), 400 μl trimethylchlorosilane, and 4.02 g (59.0 mmol) of imidazole. The mixture was warmed to 55°C over 24 h, cooled, volatile materials removed under vacuum, and the solution poured into 100 ml of water acidified to pH 6 with acetic acid. The organic phase was separated and the aqueous solution extracted with ethyl acetate, the organic phases combined, dried over sodium sulfate, and the solvent removed under reduced pressure. The yellow liquid was purified by flash chromatography over silica gel using hexane as the mobile phase to give 3.35 g (41%) of the trimethylsilyl ether.

2.2.3. Poly(oxy{methyl[4-2-hydroxyprop-2-yl)phenyl]butyl}silylene)co-oxy(dimethylsilylene)

In a 100-ml three-necked round-bottomed flask with magnetic stirring bar, two septum seals and a reflux condenser on the center neck connected to a nitrogen bubbler was added 3.35 g (12.8 mmol) of monomer and 3.14 g of poly(dimethylmethyl-hydrosiloxane) in 6 ml of benzene. The solution was heated to 55°C and 100 μl of a fresh solution of (7.8 mmol) hydrogen hexachloroplatinate (IV) hydrate in 2-propanol added. A further 400 μl of the same solution was added in increments over 48 h. The solution turned black. The disappearance of the Si–H bond was followed by NMR. Once the Si–H bond had disappeared, 500 μl (3.2 mmol) of 1-octene was added at 55°C to quench the reaction and the solution stirred for a further 6 h. The mixture was cooled and 10 g of ammonium chloride and 1 ml of 37% HCl in 10 ml of water added, the mixture stirred for 2 h, the organic phase separated and the aqueous phase filtered through a sintered glass funnel and extracted with ethyl acetate. The organic phases were combined, dried over sodium sulfate and the solvent removed under vacuum to give 6.37 g (99%) of the trimethylsilyl-protected polymer.

To the trimethylsilyl-protected polymer in 6 ml of tetrahydrofuran was added 13 ml of 1.0 M tetra-butylammonium fluoride solution in tetrahydrofuran and the mixture stirred for 6 h at room temperature. The solvent was removed under vacuum, and the residue extracted with ethyl acetate. The organic phase was washed five times with 100 ml of distilled

water, dried over anhydrous sodium sulfate, and the solvent evaporated under vacuum to give 5.40 g of PSH. ^{1}H NMR (ppm): 0.09 (singlet, 9H); 0.57 (multiplet, 2H); 1.42 (multiplet, 2H); 1.5 (singlet, 6H); 1.64 (multiplet, 2H); 2.6 (triplet, 2H); 7.15 (multiplet, 2H); and 7.39 (multiplet, 2H). ^{13}C NMR (ppm): -0.6; 0.3; 0.7; 0.9; 1.8; 16.6; 16.9; 20.7; 22.6; 24.7; 29.0; 31.6; 34.7; 35.1; 65.2; 72.4; 124.3; 126.1; 127.8; 128.1; 141.4; and 146.4. FTIR (cm^{-1}): 3600; 3500 (broad); 2963; 2929; 1409; 1366; 1260; 1168; 1085; 908; 806; 733; and 649.

2.3. Density determination

The density of the two poly(siloxane) polymers PSF6 and PSH as a function of temperature was determined using a modified Lipkin bicapillary pycnometer as described previously [35]. The data were fitted to Eq. (3)

$$\rho_t A - B(t) \qquad (3)$$

where ρ_t is the liquid density at temperature t (°C) and A and B are regression coefficients.

For PSF6 $A = 1.2208$ and $B = 12.00 \times 10^{-4}$ ($r^2 = 0.9995$ and $S_E = 0.049$) and for PSH $A = 1.0810$ and $B = 11.01 \times 10^{-4}$ ($r^2 = 0.9948$ and $S_E = 0.013$).

2.4. Determination of the gas–liquid distribution constants

The protocol used to determine the gas–liquid distribution constants is outlined in reference [36]. Briefly, all measurements were made on packed columns with a stationary phase loading of 8–20% (w/w) on Chromosorb W-AW (177–250 μm). A minimum of four phase loadings for each phase covering the above range were used to determine the gas–liquid distribution constant by averaging the individual column values when retention was solely by partitioning, found to be the general case, or by linear extrapolation to an infinite phase volume based on Eq. (4)

$$V_N^* / V_L = K_L + (\text{adsorption})(1/V_L) \qquad (4)$$

where V_N^* is the net retention volume per gram of column packing, V_L the volume of liquid phase per gram of column packing, K_L the gas–liquid dis-

tribution constant, and 'adsorption' is a composite term representing the sum of all possible interfacial adsorption retention mechanisms. The experimental conditions are arranged so that a linear extrapolation can usually be made as explained elsewhere [7,36]. The typical uncertainty in K_L is 2–5% relative standard deviation when the uncertainty in the phase loading is ±0.15% (determined by exhaustive Soxhlet extraction), carrier gas flow-rate ±0.20 ml/min, column pressure drop ±1 mmHg, column temperature ±0.2°C, and retention time ±0.02 min. The gas–liquid distribution constants at the temperatures used in the study are summarized in Table 3 for PSF6 and in Table 4 for PSH.

2.5. Instrumentation

Infrared spectra were recorded on a Nicolet 20 DX FTIR spectrometer (Madison, WI, USA) at a resolution of 2 cm^{-1} using a droplet of liquid spread between two sodium chloride plates. [1]H (300 MHz), [13]C (75.5 MHz) and [19]F (75.5 MHz) nuclear magnetic resonance spectra in chloroform-d (Cambridge Isotope Laboratories, Andover, MA, USA) were recorded on a General Electric GE-300 or GN-300 spectrometer (Freemont, CA, USA). Gas chromatographic measurements were made using a Varian 3700 gas chromatograph (Walnut Creek, CA, USA) fitted with a flame ionization detector. A mercury manometer was used to measure the column inlet pressure and a US National Institute of Standards and Technology (NIST)-certified thermometer (±0.2°C) was used to measure ambient and column temperatures.

2.6. Calculations

Multiple linear regression analysis was performed on an Epson Apex 200 computer (Epson America, Torrance, CA, USA) using the program SPSS/PC+ V5.0 (SPSS, Chicago, IL, USA). The solute descriptors used in the data analysis for the solvation parameter model (Eq. (1)) are summarized in Table 5 [5,27,37–39]. There is no significant cross-correlation among the solute descriptors (for PSF6 the highest correlation is between R_2 and π_2^H, $r = 0.52$). The solute descriptors for the solvatochromic model (Eq. (2)) are summarized in Table 6 [21,25,40].

Table 3
Gas–liquid distribution constants for various solutes on PSF6 at different temperatures (°C)

Compound	log K_L				
Temperature:	81.2	101.2	121.2	141.2	171.2
Decane	2.738	2.342	2.080	1.561	1.244
Undecane	3.063	2.636	2.330	1.817	1.471
Dodecane	3.382	2.918	2.590	2.052	1.726
Tridecane	3.696	3.209	2.840	2.279	1.939
Benzene	1.844	1.487			
Ethylbenzene	2.515	2.179		1.400	
n-Propylbenzene	2.806	2.383	2.118	1.592	1.303
n-Butylbenzene	3.129	2.672	2.381	1.819	1.560
o-Xylene	2.665	2.213	2.011	1.487	
m-Xylene	2.590	2.258	1.940	1.395	
p-Xylene	2.580	2.179	1.930	1.406	
Pentan-2-one	2.874	2.378	2.060	1.457	
Hexan-2-one	3.223	2.700	2.626	1.708	1.390
Heptan-2-one	3.557	3.000	2.630	1.979	1.644
Octan-2-one	3.884	3.296	2.890	2.225	1.853
Nonan-2-one	4.213	3.589	3.155	2.459	2.069
Cyclohexanone	3.775	3.191	2.823	2.162	1.771
Methyl hexanoate	3.491	2.946	2.577	1.925	
Ethyl hexanoate	3.769	3.179	2.794	2.124	1.784
Methyl octanoate	4.148	3.530	3.100	2.405	2.024
Methyl nonanoate	4.468	3.819	3.358	2.635	2.229
Methyl decanoate	4.800	4.115	3.615	2.864	2.438
1-Dodecyne	3.615	3.113	2.779	2.150	1.857
1,1,2,2-Tetrachloroethane	2.638	2.320	2.009	1.484	1.340
1-Bromohexane	2.680	2.295	2.055	1.505	1.245
Heptanal	3.374	2.885	2.470	1.911	
Octanal	3.697	3.180	2.733	2.176	1.782
Nonanal	4.022	3.490	2.994	2.442	1.977
Butyl acetate	3.219	2.679	2.338	1.627	1.287
Dibromomethane	1.959		1.398		
Trichloromethane	1.485	1.255	1.110		
Chlorobenzene	2.389	2.020	1.870	1.280	1.040
Bromobenzene	2.687	2.314	2.096	1.545	1.325
Iodobenzene	2.990	2.605	2.373	1.801	1.568
1,2-Dichlorobenzene	3.003	2.610	2.370	1.815	1.549
Benzonitrile	3.617	2.967	2.763	2.043	1.809
Nitrobenzene	3.522	3.090	2.750	2.106	1.891
Acetophenone	4.055	3.455	3.074	2.403	2.062
Methyl benzoate	4.012	3.374	3.030	2.382	2.019
1,4-Benzodioxan	3.938	3.385	3.013	2.335	2.052
Benzaldehyde	3.494	2.964	2.646	1.959	1.725
o-Toluidine	3.796	3.197	2.877	2.134	
p-Toluidine	3.660	3.303	2.920	2.176	1.881
Aniline	3.477	2.909	2.586	1.929	1.677
N-Methylaniline	3.654	3.161	2.740	2.216	1.794
N,N-Dimethylaniline	3.644	3.164	2.744	2.204	1.962
3-Fluoroaniline	3.310	2.929	2.590	2.047	1.648
4-Fluoroaniline	3.524	2.996	2.702	2.060	1.719
2-Chloroaniline	3.603	3.081	2.772	2.037	1.862
3-Chloroaniline	3.994	3.358	3.065	2.216	2.049
4-Chloroaniline	3.950	3.446	3.070	2.253	2.094
2-Bromoaniline	3.753	3.380	3.025	2.490	2.059
Indole	4.002	3.457	3.192	2.618	2.204

Table 4

Gas–liquid distribution constants for various solutes on PSH at 41.2°C

Compound	$\log K_{\mathrm{L}}$
Octane	2.837
Nonane	3.245
Decane	3.649
Undecane	4.053
Toluene	2.868
o-Xylene	3.395
m-Xylene	3.296
p-Xylene	3.286
Ethylbenzene	3.230
Propylbenzene	3.589
Butylbenzene	3.992
1,2,3-Trimethylbenzene	3.915
Pentan-2-one	2.870
Hexan-2-one	3.282
Heptan-2-one	3.701
1-Bromopentane	3.109
1-Bromohexane	3.523
Nitropropane	2.898
Nitropentane	3.752
n-Propanol	2.896
n-Butanol	3.343
n-Pentanol	3.788
Chlorobenzene	3.211
Bromobenzene	3.563
Iodobenzene	3.989
Propyl acetate	2.920
Butyl acetate	3.335
1-Iodoethane	2.197
1-Iodobutane	3.081
1-Octyne	3.054
1-Hexyne	2.220
Dibromomethane	2.696

Principle component factor analysis and cluster analysis were performed using the program Pirouette V1.1 (Infometrix, Seattle, WA, USA). Raw varimax rotation after mean centering was used for the principal component factor analysis [41]. For the complete link dendrogram the data were autoscaled.

3. Results and discussion

The two poly(siloxane) stationary phases are viscous liquids at room temperature and readily soluble in a variety of organic solvents. The fluorine-containing solvent, PSF6, has good column coating characteristics and an adequate operating temperature

Table 5

Solute descriptors used for the solvation parameter model (Eq. (1))

Compound	$\log L^{16}$	R_2	π_2^{H}	$\Sigma\alpha_2^{\mathrm{H}}$	$\Sigma\beta_2^{\mathrm{H}}$
Octane[a]	3.677	0	0	0	0
Nonane[a]	4.182	0	0	0	0
Decane	4.686	0	0	0	0
Undecane	5.191	0	0	0	0
Dodecane	5.696	0	0	0	0
Tridecane	6.200	0	0	0	0
Benzene	2.786	0.610	0.52	0	0.14
Toluene[a]	3.325	0.601	0.52	0	0.14
Ethylbenzene	3.778	0.613	0.51	0	0.15
n-Propylbenzene	4.230	0.604	0.50	0	0.15
n-Butylbenzene	4.730	0.600	0.51	0	0.15
o-Xylene	3.939	0.663	0.56	0	0.16
m-Xylene	3.839	0.623	0.52	0	0.16
p-Xylene	3.839	0.613	0.52	0	0.16
1,2,3-Trimethylbenzene[a]	4.565	0.728	0.61	0	0.19
Pentan-2-one	2.755	0.143	0.68	0	0.51
Hexan-2-one	3.262	0.136	0.68	0	0.51
Heptan-2-one	3.760	0.123	0.68	0	0.51
Octan-2-one	4.257	0.108	0.68	0	0.51
Nonan-2-one	4.735	0.119	0.68	0	0.51
Cyclohexanone	3.792	0.403	0.86	0	0.56
Methyl hexanoate	3.874	0.080	0.60	0	0.45
Ethyl hexanoate	4.251	0.043	0.58	0	0.45
Methyl octanoate	4.838	0.065	0.60	0	0.45
Methyl nonanoate	5.321	0.056	0.60	0	0.45
Methyl decanoate	5.803	0.053	0.60	0	0.45
Nitropropane[a]	2.894	0.242	0.95	0	0.31
Nitropentane[a]	3.938	0.212	0.95	0	0.27
1-Hexyne[a]	2.510	0.166	0.23	0.13	0.10
1-Octyne[a]	3.521	0.155	0.23	0.13	0.10
1-Dodecyne	5.657	0.133	0.23	0.13	0.10
1,1,2,2-Tetrachloroethane	3.803	0.595	0.76	0.16	0.12
1-Bromopentane[a]	3.611	0.356	0.40	0	0.12
1-Bromohexane	4.130	0.349	0.40	0	0.12
Heptanal	3.865	0.140	0.65	0	0.45
Octanal	4.361	0.160	0.65	0	0.45
Nonanal	4.856	0.150	0.65	0	0.45
Propyl acetate[a]	2.819	0.092	0.60	0	0.45
Butyl acetate	3.353	0.071	0.60	0	0.45
Iodoethane[a]	2.573	0.640	0.40	0	0.15
Iodobutane[a]	3.628	0.628	0.40	0	0.15
n-Propanol[a]	2.031	0.236	0.42	0.37	0.48
n-Butanol[a]	2.601	0.224	0.42	0.37	0.48
n-Pentanol[a]	3.106	0.219	0.42	0.37	0.48
Dibromomethane	2.886	0.714	0.67	0.10	0.10
Trichloromethane	2.480	0.425	0.49	0.15	0.02
Chlorobenzene	3.657	0.718	0.65	0	0.07
Bromobenzene	4.041	0.882	0.73	0	0.09
Iodobenzene	4.502	1.188	0.82	0	0.12
1,2-Dichlorobenzene	4.518	0.872	0.78	0	0.04
Benzonitrile	4.039	0.742	1.11	0	0.33
Nitrobenzene	4.511	0.871	1.10	0	0.27

(Cont.)

Table 5. Continued

Compound	$\log L^{16}$	R_2	π_2^H	$\Sigma\alpha_2^H$	$\Sigma\beta_2^H$
Acetophenone	4.501	0.818	1.01	0	0.49
Methyl benzoate	4.704	0.733	0.85	0	0.48
1,4-Benzodioxan	4.985	0.874	1.01	0	0.35
Benzaldehyde	4.008	0.820	1.00	0	0.39
o-Toluidine	4.442	0.966	0.92	0.23	0.45
p-Toluidine	4.452	0.923	0.95	0.23	0.45
Aniline	3.993	0.955	0.96	0.26	0.41
N-Methylaniline	4.494	0.948	0.94	0.17	0.47
N,N-Dimethylaniline	4.701	0.957	0.81	0	0.41
3-Fluoroaniline	3.988	0.749	1.08	0.30	0.36
4-Fluoroaniline	4.007	0.760	1.09	0.28	0.40
2-Chloroaniline	4.674	1.033	0.92	0.25	0.31
3-Chloroaniline	4.909	1.053	1.10	0.30	0.30
4-Chloroaniline	4.889	1.060	1.10	0.30	0.30
2-Bromoaniline	5.104	1.070	0.98	0.31	0.31
Indole	5.505	1.200	1.12	0.44	0.22

[a] Used only to characterize PSH at 41.2°C.

Table 6
Solute descriptors used for Carr's model (Eq. (2))

Compound	$\log L^{16c}$	δ_2	π_2^c	α_2^c	β_2^c
Octane[a]	3.677	0	−0.12	0	0
Nonane[a]	4.176	0	−0.12	0	0
Decane	4.685	0	−0.11	0	0
Undecane	5.191	0	−0.10	0	0
Dodecane	5.696	0	−0.09	0	0
Tridecane	6.200	0	−0.08	0	0
Benzene	2.792	1	0.29	0	0.10
Ethylbenzene	3.785	1	0.30	0	0.11
Propylbenzene	4.239	1	0.30	0	0.11
Butylbenzene	4.714	1	0.30	0	0.11
o-Xylene	3.947	1	0.31	0	0.12
m-Xylene	3.868	1	0.29	0	0.12
p-Xylene	3.867	1	0.28	0	0.12
Hexan-2-one	3.262	0	0.39	0	0.48
Heptan-2-one	3.766	0	0.41	0	0.48
Octan-2-one	4.257	0	0.43	0	0.48
Nonan-2-one	4.755	0	0.44	0	0.48
Cyclohexanone	3.580	0	0.59	0	0.56
Heptanal	3.860	0	0.38	0	0.39
Butyl acetate	3.379	0	0.33	0	0.48
Di-n-butyl ether	3.954	0	0.04	0	0.29
Trichloromethane	2.478	0.5	0.27	0.16	0.04
Chlorobenzene	3.630	1	0.44	0	0.09
Bromobenzene	4.022	1	0.51	0	0.10
Iodobenzene	4.505	1	0.59	0	0.09
1,2-Dichlorobenzene	4.453	1	0.56	0	0.09
Acetophenone	4.458	1	0.80	0	0.49
Benzonitrile	3.913	1	0.85	0	0.40
Nitrobenzene	4.433	1	0.91	0	0.21
Benzaldehyde	3.935	1	0.75	0	0.42
Aniline	3.934	1	0.76	0.20	0.42
N-Methylaniline	4.492	1	0.70	0.14	0.31
N,N-Dimethylaniline	4.753	1	0.57	0	0.26
Pyridine	2.969	1	0.60	0	0.90
n-Propanol[a]	1.975	0	0.30	0.32	0.45
n-Butanol[a]	2.539	0	0.30	0.31	0.45
n-Pentanol[a]	3.057	0	0.32	0.32	0.45
n-Propyl acetate[a]	2.861	0	0.32	0	0.45
Nitropropane[a]	2.773	0	0.65	0	0.18

[a] Used only to characterize PSH at 41.2°C.

range for the proposed studies. No upper temperature limit was established for PSF6, but it was routinely used over the temperature range of 50–200°C and provided about 1500–1800 theoretical plated per meter (a figure similar to conventional poly(siloxane) stationary phases prepared with the same support material). An approximate composition (Fig. 2) and molecular weight of 4700 was estimated from the integration of the proton NMR signals and a knowledge of the molecular weight of the starting materials. Based on these results we estimate that PSF6 contains about 70% dimethylsiloxane groups, 26% methylsiloxane groups with the fluorine-containing alcohol substituent attached, and 4% methyloctylsiloxane groups. The PSH polymer had a similar composition (28% methylsiloxane groups with the alcohol substituent attached) and a molecular weight of about 3660. PSH possessed unfavorable thermal properties for use in gas chromatography. An upper column temperature limit of 60°C was established by decomposition. Heating the polymer in a closed container at 100°C overnight resulted in the separation of a fine white powder and disappearance of the isopropanol group in the NMR, with an additional signal appearing in the vinylic region of the spectrum. We did not pursue the nature of the mechanism further, but it seems plausible that the alcohol loses water at quite low temperatures with the formation of vinylic groups that undergo some crosslinking to form an insoluble residue. The PSH polymer was prepared for comparison to PSF6, to demonstrate the singular importance of employing an alcohol with strongly electronegative groups as near neighbors, and is used to this end in these studies, although comments are restricted to a single temperature by its unfavorable thermal properties. The peak area response observed for some alcohols and phenols was less than expected when chromato-
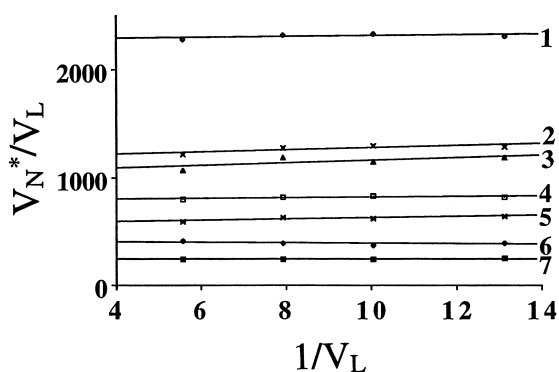
Fig. 4. Plot of V_N^*/V_L against $1/V_L$ for a number of varied solutes on PSF6 at 121.2°C. Solute identification: (1) methyl nonanoate; (2) acetophenone; (3) 3-chloroanaline; (4) octan-2-one; (5) nitrobenzene; (6) dodecane; and (7) butylbenzene.

graphed on PSF6, but not PSH, possibly due to chemical reactions. Solutes belonging to these groups were not used in the characterization studies for PSF6.

For the unbiased estimate of the solvation properties of PSF6 and PSH results are reported in the form of the gas–liquid distribution constant corrected for contributions from interfacial adsorption. The dominant retention mechanism for PSF6 is gas–liquid partitioning with a small contribution from interfacial adsorption, as indicated in the representative plots in Fig. 4. The slope of the plots is indicative of the general retention mechanism with a zero slope characteristic of pure gas–liquid partitioning and a positive slope of a residual contribution from interfacial (gas–liquid or gas–solid) adsorption

[7,42–44]. The intercept of the plots at $1/V_L = 0$ corresponds to the gas–liquid distribution constant independent of interfacial adsorption. A comparison of the intercept value to the magnitude of the slope is an indication that interfacial adsorption for PSF6 is never more than a minor retention mechanism for the varied solutes indicated in Table 3.

The solvation properties of the poly(siloxane) solvents were established by fitting the gas–liquid distribution constants in Tables 3 and 4 to the solvation parameter model (Eq. (1)), giving the characteristic system constants and statistics for the fit summarized in Table 7. The standard error in the estimate of log K_L from 0.04 to 0.07 log units and the general statistics indicate that the model provides a good representation of the experimental data. For interpretive purposes we will look at the general properties of the two stationary phases first and then comment on the influence of temperature on their solvation behavior.

PSF6 is a strong hydrogen-bond acid solvent as indicated by the magnitude of the b system constant. It has no significant hydrogen-bond basicity since the a constant is statistically insignificant. The solvent has a modest capacity for dipole-type interactions and, as expected for a fluorine-containing solvent, interactions involving n- and π-electron pairs are repulsive in nature. From the values for the I system constant and the equation constant, c, part of which is related to ease of cavity formation, PSF6 has a low cohesive energy and cavity formation is relatively easy. PSF6 is a strong hydrogen-bond acid stationary phase with good selectivity, since its relative capaci-

Table 7
System constants from the solvation parameter model (Eq. (1)) for PSF6 and PSH

Temperature (°C)	System constants						Statistics[a]			
	l	r	s	a	b	c	ρ	S_E	F	n
PSF6										
81.2	0.66 (0.01)	−0.50 (0.06)	0.89 (0.09)	0	1.79 (0.11)	−0.40 (0.07)	0.995	0.073	1084	53
101.2	0.60 (0.01)	−0.38 (0.04)	0.76 (0.06)	0	1.52 (0.07)	−0.48 (0.04)	0.997	0.047	1787	52
121.2	0.54 (0.01)	−0.36 (0.05)	0.82 (0.07)	0	1.11 (0.08)	−0.51 (0.05)	0.994	0.057	1067	53
141.2	0.49 (0.01)	−0.28 (0.04)	0.63 (0.06)	0	0.96 (0.07)	−0.76 (0.05)	0.993	0.050	792	51
171.2	0.46 (0.01)	−0.23 (0.04)	0.68 (0.06)	0	0.69 (0.07)	−0.92 (0.06)	0.992	0.043	598	45
PSH										
41.2	0.83 (0.02)	0	0.43 (0.04)	1.93 (0.10)	1.14 (0.07)	−0.26 (0.07)	0.995	0.048	736	32

[a] ρ, multiple correlation coefficient; S_E, standard deviation in the estimate; F, Fischer F-statistic; n, number of solutes; and the numbers in ( ) are the standard deviation in the system constants.

ty for other polar interactions (a/b, s/b, and r/b) are either non-existent or modest, with favorable general separation characteristics for small molecules due to its low cohesion. By contrast, PSH is simultaneously both a strong hydrogen-bond acid and a base, and since the a system constant is significantly larger than the b system constant, we can safely conclude that it is a stronger hydrogen-bond base than hydrogen-bond acid. It is weakly dipolar (small s system constant) and has no capacity for lone pair electron interactions, at least at 41.2°C, since the r system constant is statistically insignificant. Similar to PSF6 it is a solvent of low cohesion. In general terms, the introduction of fluorine for hydrogen in the isopropanol subunit of the stationary phase has a dramatic effect on its solvation properties. In particular, there is a large increase in the hydrogen-bond acidity of the solvent accompanied by a diminished capacity to function as a hydrogen-bond base, an increase in the capacity of the solvent for dipole-type interactions, and a change in the character of the solvent with regard to lone pair electron interactions.

Since all polar interactions are temperature dependent, the influence of temperature on solvation properties is an important consideration for the use of a stationary phase in gas–liquid chromatography. These features are best illustrated graphically (Fig. 5). Over the temperature range studied for PSF6, there is a significant decline in the contribution of hydrogen-bond acidity and lone pair electron repulsion interactions of the stationary phase, and a modest decline in its capacity for dipole-type interactions. These changes in system constants with temperature are approximately linear. By extrapolation, the b system constant would reach zero at a temperature of about 210°C and it would have a value of about 2.30 at 41.2°C. The temperature of 171.2°C was the highest practical experimental temperature for which meaningful gas–liquid distribution constants could be obtained for a significant number of the solutes in Table 5 used to define the system constants. Even providing that there may be some reasonable objections to the extrapolations used it is beyond doubt that PSF6 retains its hydrogen-bond acid character over a sufficiently wide temperature range to be a useful stationary phase for separations performed between room temperature and 200°C. If 2.30 is a realistic estimate for the b system constant
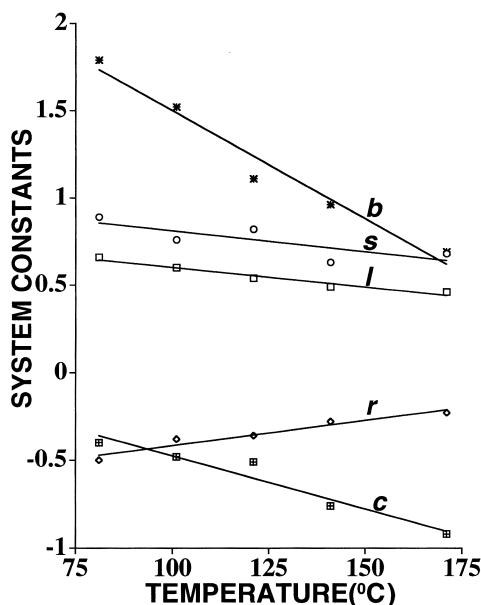

Fig. 5. Plot of the system constants derived from the solvation parameter model as a function of temperature for PSF6.

at 41.2°C then PSF6 is a significantly stronger hydrogen-bond acid than PSH ($b = 1.14$).

The breakdown of the contribution of individual intermolecular interactions to retention provides a clear indication of the dominant forces responsible for selective solvation in the PSF6 stationary phase. By way of example we will consider octan-2-one (Fig. 6) and acetophenone (Fig. 7) only. The opposing contributions from cavity formation in the stationary phase and dispersion interactions between the solute and stationary phase are represented by the sum of $(c + l \log L^{16})$ on the plots. This cannot be an exact assessment since the c constant contains contributions related to the lack of fit for the model and possibly scaling errors in the solute descriptors but, as demonstrated in previous studies, the sum term is a better representation of the cavity and dispersion contributions than the $l \log L^{16}$ term alone [13,16,17,27,39]. For now, we have no exact method to dissect the sum $\Sigma(c + l \log L^{16})$ into precisely defined contributions of cavity formation and dispersion interactions [41]. For octan-2-one and acetophenone the dominant interaction between the solutes and PSF6 is dispersion interactions, which easily exceed the opposing requirement for cavity
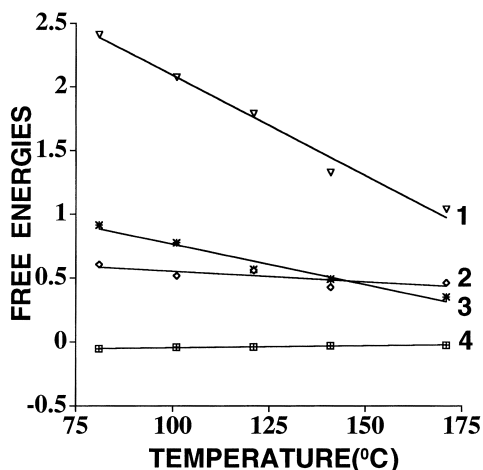
Fig. 6. Contribution of dimensionless free energies for individual intermolecular interactions to the retention of octan-2-one on PSF6 as a function of temperature. Identification: (1) cavity formation and dispersion interactions; (2) dipole-type interactions; (3) solute hydrogen-bond base–solvent hydrogen-bond acid interactions; and (4) lone pair-lone pair electron repulsion.

formation in the stationary phase. Acetophenone has an appreciably greater capacity for interactions of a dipole-type than octan-2-one (compare π_2^H terms in Table 5) and similar hydrogen-bond basicity. This is reflected in the relative difference in the contribution
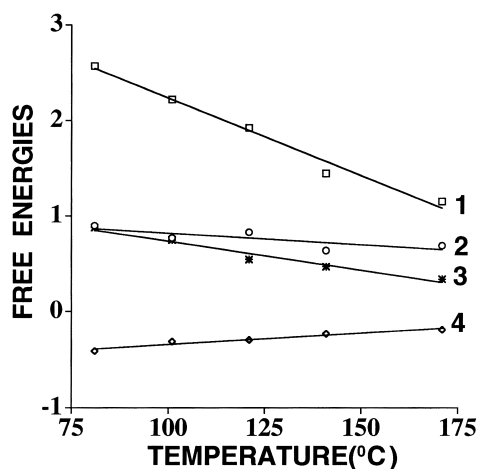

Fig. 7. Contribution of dimensionless free energies for individual intermolecular interactions to the retention of acetophenone on PSF6 as a function of temperature. Identification: (1) cavity formation and dispersion interactions; (2) dipole-type interactions; (3) solute hydrogen-bond base–solvent hydrogen-bond acid interactions; and (4) lone pair-lone pair electron repulsion.

of dipole-type and solute hydrogen-bond base–solvent hydrogen-bond acid interactions to retention observed and the change in the relative importance of these two interactions with temperature. Solute hydrogen-bond base–solvent hydrogen-bond acid interactions exhibit a greater temperature dependence than dipole-type interactions, such that for octan-2-one hydrogen-bond interactions are more important as polar contributions to retention at low temperatures and dipole-type interactions at higher temperatures. Lone pair–lone pair electron repulsion is only a minor contributing factor to retention for both compounds. Note that since the a system constant is zero, it is not necessary to consider solute hydrogen-bond acid–solvent hydrogen-bond base interactions, even for strong solute hydrogen-bond acids, because PSF6 lacks the complementary characteristic properties to participate in these interactions.

The different blends of covalent and electrostatic interactions in hydrogen-bond complexation make the promulgation of a universal scale of solvent hydrogen-bond acidity somewhat difficult [9,45,46]. Carr and co-workers [21,24,25] have defined a different scale of solute hydrogen-bond basicity to that used in the solvation parameter model based on 4-dodecyl-α,α-bis(trifluoromethyl)benzyl alcohol as the reference hydrogen-bond acid solvent for use in the model described by Eq. (2). Since the numerical values of the solute descriptors are different to those employed in the solvation parameter model differences in the numerical values of the system constants are to be expected, but the trends predicted by both models should be consistent. This is confirmed by the data in Table 8, obtained by fitting the gas–liquid distributions constants for PSF6 and PSH to Carr's model, for those solutes we had descriptors available. The Carr descriptors and the Abraham descriptors account for solvation on PSF6 almost equally well. The slightly better statistical fit for Carr's model is not too surprising since Carr's β_2^c term has been trained on a similar acidic stationary phase and the Carr descriptors would be expected to be better suited to account for solvation on a very similar phase.

From previous studies we have system constants available for 12 common poly(siloxane) stationary phases at 121.2°C, summarized in Table 9 [7,19,33]. The system constants representing polar interactions

Table 8
System constants from Carr's model (Eq. (2)) for PSF6 and PSH with comparison to the statistical fit to Abraham's model (Eq. (1)) for the same solutes

Temperature (°C)	System constants						Statistics						
	Carr's model						Carr's model				Abraham's model		
	l	d	s	a	b	c	ρ	S_E	F	n	ρ	S_E	F
PSF6													
81.2	0.65 (0.01)	−0.17 (0.02)	0.62 (0.05)	0	2.24 (0.06)	−0.23 (0.05)	0.998	0.042	1704	33	0.996	0.057	815
101.2	0.59 (0.01)	−0.12 (0.03)	0.54 (0.05)	0	1.91 (0.06)	−0.36 (0.06)	0.997	0.045	920	33	0.997	0.045	1068
121.2	0.53 (0.01)	−0.08 (0.02)	0.51 (0.04)	0	1.63 (0.05)	−0.37 (0.05)	0.996	0.043	969	33	0.995	0.052	611
141.2	0.46 (0.01)	−0.12 (0.02)	0.51 (0.05)	0	1.18 (0.05)	−0.53 (0.05)	0.996	0.039	801	32	0.995	0.041	454
171.2	0.51 (0.02)	−0.07 (0.03)	0.59 (0.07)	0	1.20 (0.09)	−1.12 (0.09)	0.990	0.058	304	30	0.990	0.046	270
PSH													
41.2	0.79 (0.01)	−0.12 (0.01)	0.81 (0.03)	2.29 (0.05)	0.78 (0.04)	0.01 (0.04)	0.999	0.018	1929	23			

cover a wide numerical range (with the exception of the b system constant which is zero in all cases). We can use these stationary phases as a basis set to determine the usefulness of PSF6 as an additional stationary phase for gas–liquid chromatography. We can evaluate the contribution from cavity formation and dispersion interactions, as before, using the sum

Table 9
System constants extracted from the solvation parameter model at 121.2°C for common poly(siloxane) stationary phases ($b = 0$ in all cases)

Solvent[a]	System constants				
	l	r	s	a	c
SE-30	0.50	0.02	0.19	0.13	−0.19
OV-3	0.50	0.03	0.33	0.15	−0.18
OV-7	0.51	0.06	0.43	0.17	−0.23
OV-l1	0.52	0.10	0.54	0.17	−0.30
OV-17	0.52	0.07	0.65	0.26	−0.37
OV-22	0.48	0.20	0.66	0.19	−0.33
OV-25	0.47	0.28	0.64	0.18	−0.27
OV-105	0.50	0	0.36	0.41	−0.20
OV-225	0.47	0	1.23	1.07	−0.54
OV-275	0.29	0.21	2.08	1.99	−0.91
QF-1	0.42	−0.45	1.16	0.19	−0.27
OV-330	0.48	0.10	1.06	1.42	−0.43

[a] SE-30, poly(dimethylsiloxane); OV-3, OV-7, OV-11, and OV-17 are poly(methylphenylsiloxane)s containing 10, 20, 35 and 50 mol.% phenyl groups, respectively; OV-22 and OV-25 are poly-(methylphenyldiphenylsiloxane)s containing 65 and 75 mol.% phenyl groups, respectively; OV-105, poly(cyanopropyl-methyldimethylsiloxane); OV-225, poly(cyanopropylmethyl-phenylmethylsiloxane); OV-275, poly(dicyanoallylsiloxane); QF-1, poly(trifluoropropylmethylslloxane); and OV-330, poly(di-methylsiloxane)/Carbowax copolymer.

term $\Sigma(c + l \log L^{16})$ calculated for decane (Table 10). The cavity formation–dispersion interaction term for the poly(dimethylsiloxane), poly-(methylphenylsiloxane) and PSF6 are numerically similar, indicating a comparable difficulty in cavity formation, if it is assumed to a first approximation, that the dispersion interactions are proportional to the solute's volume. For the poly(methylphenyldi-phenylsiloxane)s and the poly(siloxane)s containing substituents with dipolar functional groups the cavity term is less favorable due to stronger solvent–solvent intermolecular interactions (see the data for OV-275 for an extreme example). PSF6, then, has a low cohesive energy, similar to the least polar poly(silox-ane) stationary phases.

Table 10
Contribution of cavity formation and dispersion interactions to solution of decane in the poly(siloxane) stationary phases at 121.2°C

Solvent	c	$l \log L$	$\Sigma(c + l \log L^{16})$
OV-3	−0.181	2.357	2.176
OV-7	−0.231	2.390	2.159
SE-30	−0.194	2.334	2.140
OV-105	−0.203	2.324	2.121
OV-11	−0.303	2.418	2.115
OV-17	−0.372	2.427	2.055
PSF6	−0.512	2.540	2.028
OV-25	−0.273	2.212	1.939
OV-22	−0.328	2.259	1.931
OV-330	−0.430	2.254	1.824
QF-1	−0.269	1.963	1.694
OV-225	−0.541	2.184	1.643
OV-275	−0.909	1.378	0.469

Table 11
Summary of results from principal component analysis of the selectivity space for the 13 poly(siloxane) stationary phases

Principal component	Variance (%)	Cumulative variance (%)	
1	75.2	75.2	
2	16.9	92.1	
3	5.1	97.2	
4	2.5	99.7	
5	0.2	99.9	
Loadings for principal components			
System constant	PC 1	PC 2	PC 3
l	−0.066	0.006	0.123
r	0.036	−0.425	0.326
s	0.603	0.374	−0.556
a	0.759	−0.270	0.450
b	−0.059	0.765	0.595
c	−0.228	−0.184	−0.111

For a more general view of the capacity of the poly(siloxane) stationary phases for selective polar interactions we applied principal component factor analysis and cluster analysis to the data in Table 9. The loadings for the principal components are summarized in Table 11. The loadings indicate how much each variable (system constant) contributes to the principal component (interaction) responsible for the solvation mechanism. With two principal components we can explain 92.1% of the total variance giving the score plot in Fig. 8. Principal component 1 is influenced mainly by the capacity of the stationary phase for dipole-type and hydrogen-bond base interactions, and principal component 2 by the stationary phase hydrogen-bond acidity, dipole character, and capacity for lone pair electron interactions. Viewing
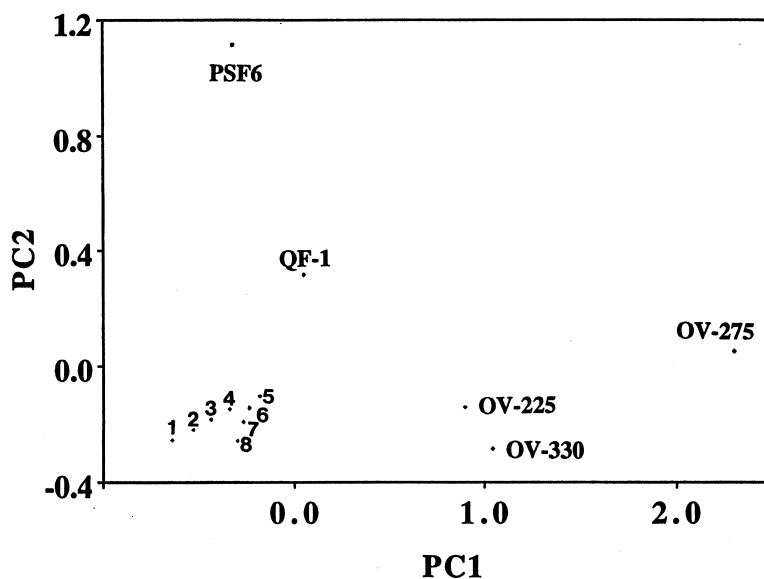

Fig. 8. Score plot for the principal component factor analysis of the system constants for the poly(siloxane) stationary phases. Identification: (1) SE-30; (2) OV-3; (3) OV-7; (4) OV-11; (5) OV-17; (6) OV-22; (7) OV-25; and (8) OV-105.
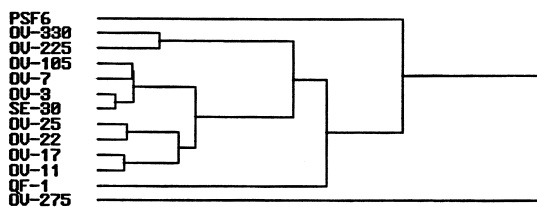
Fig. 9. Complete link dendrogram from cluster analysis of the system constants for the poly(siloxane) stationary phases.

4. Conclusions

PSF6 is the first useful high-temperature hydrogen-bond acid stationary phase for methods development in gas–liquid chromatography. As well as strong hydrogen-bond acidity it has low cohesion, intermediate dipolarity and zero hydrogen-bond basicity. The increased hydrogen-bond acidity to external solutes of PSF6 over a PSH is due to (i) the inductive effect of fluorine atoms increasing the intrinsic hydrogen-bond acidity and decreasing the intrinsic hydrogen-bond basicity, but (ii) the effect of this is to reduce the internal hydrogen-bonding, and so PSF6 appears an even stronger hydrogen-bond acid to an external solute hydrogen-bond base. The capacity of PSF6 for solvent hydrogen-bond acid–solute hydrogen-bond base interactions is temperature dependent with a useful temperature range up to about 200°C. Fluorine-containing alcohols (and also possibly phenols) represent a new opening in poly(siloxane) chemistry for the synthesis of a broader range of selective stationary phases, of which PSF6 is the first of these materials. A comparison of its solvent properties with commonly used poly(siloxane) phases indicates that it is a singular solvent with properties not duplicated by existing phases.

the selectivity space created in this way, the poly(dimethylsiloxane), poly(methylphenylsiloxane) and poly(methylphenyldiphenylsiloxane) phases are tightly clustered close to the origin of the plot and provide very limited possibilities for selectivity optimization. The most singular solvents, located at the extremes of the axes, are PSF6 and OV-275. These phases are most different from each other and the other poly(siloxane) phases. Also, since most of the selectivity space is vacant, an opportunity exists to design new poly(siloxane) phases with a broader range of selectivity characteristics through variation in composition employing different blends of dipolar and hydrogen-bond acid/base functional groups. Selectivity may also be varied by employing different fluorine-containing alcohol or phenol substituent groups, since both the number and position of the fluorine atoms influence the hydrogen-bond acidity, basicity and dipole character of the phase. In the absence of PSF6 the selectivity space would contract significantly indicating that PSF6 is fulfilling a need that other common poly(siloxane) phases do not.

The output from cluster analysis is obtained in the form of a dendrogram (Fig. 9). Descendants which are most similar to each other are found on the left-hand side of the plot and those with the fewest features in common are connected at the right-hand side. PSF6, OV-275 and QF-1 are identified as singular stationary phases whose properties, in large part, cannot be duplicated by other phases taken for analysis. For methods development using the poly(siloxane) phases the greatest differences in selectivity is achieved using PSF6, OV-275, QF-1, OV-225 (or OV-330), OV-25 (or OV-22), and one of (OV-105, OV-7, OV-3, SE-30, OV-17, or OV-11).

References

[1] C.F. Poole, S.K. Poole, Chromatography Today, Elsevier, Amsterdam, The Netherlands, 1991, pp. 108–118.

[2] H. Rotzsche, Stationary Phases in Gas Chromatography, Elsevier, Amsterdam, The Netherlands, 1991.

[3] K.K. Unger (Ed.), Packings and Stationary Phases in Chromatographic Techniques, Marcel Dekker, New York, 1990, pp. 87–234.

[4] G.E. Baiulescu, V.A. Ilie, Stationary Phases in Gas Chromatography, Pergamon, Oxford, 1975.

[5] M.H. Abraham, Chem. Soc. Rev. 22 (1993) 73.

[6] R.W. Taft, M. Berthelot, C. Laurence, A.J. Leo, Chem. Tech. (1996) 20.

[7] C.F. Poole, T.O. Kollie, S.K. Poole, Chromatographia 34 (1992) 281.

[8] P.W. Carr, Microchem. J. 48 (1993) 4.

[9] M.H. Abraham, in: P. Politzer, J.S. Murray (Eds.), Quantitative Treatments of Solute/Solvent Interactions, Elsevier, Amsterdam, 1994, pp. 83–134.

[10] M.H. Abraham, H.S. Chadha, in: V. Pliska, B. Testa, H. van de Waterbeemd (Eds.), Lipophilicity in Drug Action and Toxicology, VCH, Weinheim, Germany, 1996, pp. 311–337.

[11] M.H. Abraham, G.S. Whiting, R.M. Doherty, W.J. Shuely, J. Chromatogr. 518 (1990) 329.

[12] M.H. Abraham, G.S. Whiting, R.M. Doherty, W.J. Schuely, J. Chem. Soc. Perkin Trans. 2 (1990) 1451.

[13] M.H. Abraham, G.S. Whiting, R.M. Doherty, W.J. Shuely, J. Chromatogr. 587 (1991) 229.

[14] M.H. Abraham, G.S. Whiting, R.M. Doherty, W.J. Shuely, J. Chem. Soc. Perkin Trans. 2 (1990) 1851.

[15] M.H. Abraham, Anal. Chem. 69 (1997) 613.

[16] T.O. Kollie, C.F. Poole, M.H. Abraham, G.S. Whiting, Anal. Chim. Acta 259 (1992) 1.

[17] C.F. Poole, T.O. Kollie, Anal. Chim. Acta 282 (1993) 1.

[18] S.K. Poole, C.F. Poole, Analyst 120 (1995) 289.

[19] S.K. Poole, C.F. Poole, J. Chromatogr. A 697 (1995) 415.

[20] M.H. Abraham, G.S. Whiting, J. Andonian-Haftvan, J.W. Steed, J.W. Grate, J. Chromatogr. 588 (1991) 361.

[21] J. Li, Y. Zhang, P.W. Carr, Anal. Chem. 64 (1992) 210.

[22] J. Li, Y. Zhang, A.J. Dallas, P.W. Carr, J. Chromatogr. 550 (1991) 101.

[23] J. Li, A.J. Dallas, P.W. Carr, J. Chromatogr. 517 (1990) 103.

[24] J. Li, Y. Zhang, H. Ouyang, P.W. Carr, J. Am. Chem. Soc. 114 (1992) 9813.

[25] J. Li, Y. Zhang, P.W. Carr, Anal. Chem. 65 (1993) 1969.

[26] M.H. Abraham, I. Hamerton, J.B. Rose, J.W. Grate, J. Chem. Soc. Perkin Trans. 2 (1991) 1417.

[27] M.H. Abraham, J. Andonian-Haftvan, I. Hamerton, C.F. Poole, T.O. Kollie, J. Chromatogr. 646 (1993) 351.

[28] M.H. Abraham, J. Andonian-Haftvan, C.M. Du, V. Diart, G.S. Whiting, J.W. Grate, R.A. McGill, J. Chem. Soc. Perkin Trans. 2 (1995) 369.

[29] J.W. Grate, A. Snow, D.S. Ballantine, H. Wohltjen, M.H. Abraham, R.A. McGill, P. Sasson, Anal. Chem. 60 (1988) 869.

[30] A.W. Snow, L.G. Sprague, R.L. Soulen, J.W. Grate, H.J. Wohltjen, J. Appl. Poly. Sci. 43 (1991) 1659.

[31] J.W. Barlow, P.E. Cassidy, D.R. Lloyd, C.-J. You, Y. Chang, P.C. Wong, J. Noriyan, Poly. Eng. Sci. 27 (1987) 703.

[32] J.W. Grate, M.H. Abraham, Sensors Actuators B 3 (1991) 85.

[33] S.K. Poole, K.G. Miller, C.F. Poole, J. Microcol. Sep. 7 (1995) 497.

[34] P.E. Peterson, D.M. Cheveli, J. Org. Chem. 33 (1968) 976.

[35] K.G. Furton, C.F. Poole, J. Chromatogr. 399 (1987) 47.

[36] S.K. Poole, C.F. Poole, J. Chromatogr. 500 (1990) 329.

[37] M.H. Abraham, J. Phys. Org. Chem. 6 (1993) 660.

[38] M.H. Abraham, J. Chromatogr. 644 (1993) 95.

[39] G. Park, C.F. Poole, J. Chromatogr. A 726 (1996) 141.

[40] J. Li, P.W. Carr, J. Chromatogr. A 659 (1994) 367.

[41] S.K. Poole, C.F. Poole, J. Chromatogr. A 697 (1995) 429.

[42] B.R. Kersten, C.F. Poole, J. Chromatogr. 399 (1987) 1.

[43] C.F. Poole, S.K. Poole, Chem. Rev. 89 (1989) 377.

[44] S.K. Poole, T.O. Kollie, C.F. Poole, J. Chromatogr. A 664 (1994) 229.

[45] P.-C. Maria, J.-F. Gal, J. de Franceschi, E. Fargin, J. Am. Chem. Soc. 109 (1987) 483.

[46] M.H. Abraham, P.L. Grellier, D.V. Prior, J.J. Morris, P.J. Taylor, P.-C. Maria, J.-F. Gal, J. Phys. Org. Chem. 2 (1989) 243.